Open access • Journal Article • DOI:10.1109/JQE.2012.2233462

High-Gain InAs Avalanche Photodiodes — Source link

Wenlu Sun, Zhiwen Lu, Xiaoguang Zheng, Joe C. Campbell ...+3 more authors

Institutions: University of Virginia, University of Texas at Austin

Published on: 21 Jan 2013 - IEEE Journal of Quantum Electronics (IEEE)

Topics: Avalanche photodiode, Single-photon avalanche diode, Depletion region and Photodetector

High-Gain InAs Avalanche Photodiodes

Wenlu Sun, Zhiwen Lu, Xiaoguang Zheng, Joe C. Campbell, *Member, IEEE*, Scott J. Maddox, Hari P. Nair, and Seth R. Bank, *Senior Member, IEEE*

***Abstract*— We report two InAs avalanche photodiode structures with very low background doping in the depletion region. Uniform electric fields and thick depletion regions have been achieved. Excess noise measurements are consistent with k~0 and gain as high as 70 at room temperature is observed. The measured gain-bandwidth product is > 300 GHz. All measurements are consistent with Monte Carlo simulations.**

***Index Terms*— Avalanche photodiode, excess noise, gain-bandwidth product, Monte Carlo simulation.**

I. Introduction

AVALANCHE photodiodes (APDs) can improve receiver sensitivity and detect weak photon flux owing to their internal gain. They have been widely used in short-wave and mid-wave infrared detection systems, such as imaging, LIDAR detection, and communications. The statistical nature of impact ionization in APDs generates excess shot noise. According to the local-field model [1] the noise power spectral density, ϕ for mean gain, <M>, and mean photocurrent, $<I_{ph}>$, is given by the expression $\phi = 2q<I_{ph}><M>^2F(M)$. F(M) is the excess noise factor, which arises from the random nature of impact ionization. Under the conditions of uniform electric fields and pure electron injection, the excess noise factor can be expressed in terms of <M> and the ratio of the electron and hole ionizaiton coefficients, k, as $F(M) = <M^2>/<M>^2 = k\bullet<M> + (1-k)(2-1/<M>)$. InGaAs is a material that is frequently used for short-wave infrared detection, however, its cut-off wavelength (~1.65 μm) limits its suitability for mid-wave applications. The low bandgap of $Hg_{0.7}Cd_{0.3}Te$ (~0.29 eV) provides good mid-wave response. A particularly attractive feature of $Hg_{0.7}Cd_{0.3}Te$ is that k~0 since only electrons initiate impact ionization. Hence the excess noise factor is <2 and independent of gain. However, the low bandgap also results in relatively high dark current at room temperature, which necessitates operation at low temperature. Recently, InAs APDs have also demonstrated k~0 with moderately low dark current at room temperature [2]–[5]. InAs APDs with thick multiplication regions have also exhibited high gain at low bias [3], which is beneficial for integration with Read Out-Integrated Circuits (ROICs). To design a high-gain InAs APD with a thick gain region, low background doping is essential in order to realize complete depletion and a uniform, i.e. "flat," electric field profile. In this paper, we report two high-gain InAs APD structures employing a 6 μm-thick i region with low background doping concentration. Monte Carlo simulation is employed to study the impact ionization properties of these APDs. Good agreement is obtained between the simulations and measurements [3]–[7].

TABLE I
Parameters Used in Monte Carlo Simulation

Material Parameters	Γ	L	X
Energy band-gap (eV)	0.417	1.133	1.433
Electron effective mass (m^*/m_0)	0.026	0.072	0.224
Threshold energy of impact ionization (eV)	0.82		
Longitudinal sound velocity (m/s)	4620		
Static dielectric constant	15.15		
High frequency dielectric constant	12.3		
Accoustic phonon energy (meV)	11.0		
Optical phonon energy (meV)	24.3		
Intervalley phonon energy (meV)	13.2		
Intervalley deformation potential (eV/m)	1.07×10^{11}		

II. Monte Carlo Simulation

The Monte Carlo tool that was used in this work is similar to the model in [8], [9], which is based on a physical-level description of carrier transport. The model uses a simplified non-parabolic band structure that includes the Γ, L, and X valleys in the conduction band, and heavy-hole, light-hole, and split-off valence bands. For carrier scattering, we include impurity scattering, acoustic and optical phonon scattering, and more importantly, impact ionization scattering calculated using the Keldysh formula [10]. Some important model parameters are listed in Table 1. Simulated electron drift velocities in bulk InAs at different electric field strengths agree with those reported in [11], as shown in Fig. 1. The decrease of the electron drift velocity at higher field is attributed to intervalley scattering. The saturation velocity of electrons in InAs is demonstrated to be close to 1×10^5 m/s, which is faster than that of InGaAs.

The scattering parameters were determined by simulating p-i-n structures with the i-region thicknesses reported in [3], which are 0.9 μm, 1.9 μm, and 3.5 μm. Pure electron injection is assumed for these simulations. The simulated gain agrees

Manuscript received October 16, 2012; revised December 4, 2012; accepted December 7, 2012. Date of publication December 11, 2012; date of current version January 9, 2013. This work was supported by the Army Research Office, under Award W911NF-10-1-0391, monitored by Dr. B. Clark.

W. Sun, Z. Lu, X. Zheng, and J. C. Campbell are with the Department of Electrical and Computer Engineering, University of Virginia, Charlottesville, VA 22904 USA (e-mail: ws8zp@virginia.edu; zl2a@cms.mail.virginia.edu; xz7u@virginia.edu; jcc7s@virginia.edu).

S. J. Maddox, H. P. Nair, and S. R. Bank are with the Department of Electrical and Computer Engineering, University of Texas at Austin, Austin, TX, 78758 USA (e-mail: smaddox@utexas.edu; hnair@mail.utexas.edu; sbank@ece.utexas.edu).

Color versions of one or more of the figures in this paper are available online at http://ieeexplore.ieee.org.

Digital Object Identifier 10.1109/JQE.2012.2233462

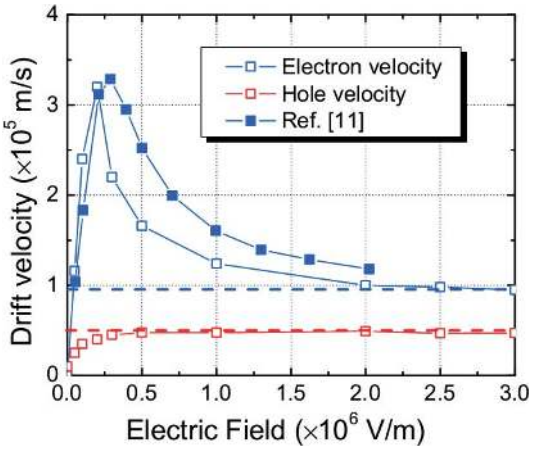

Fig. 1. Simulated electron drift velocity of InAs (open symbol), compared to the data in [11] (closed symbol).

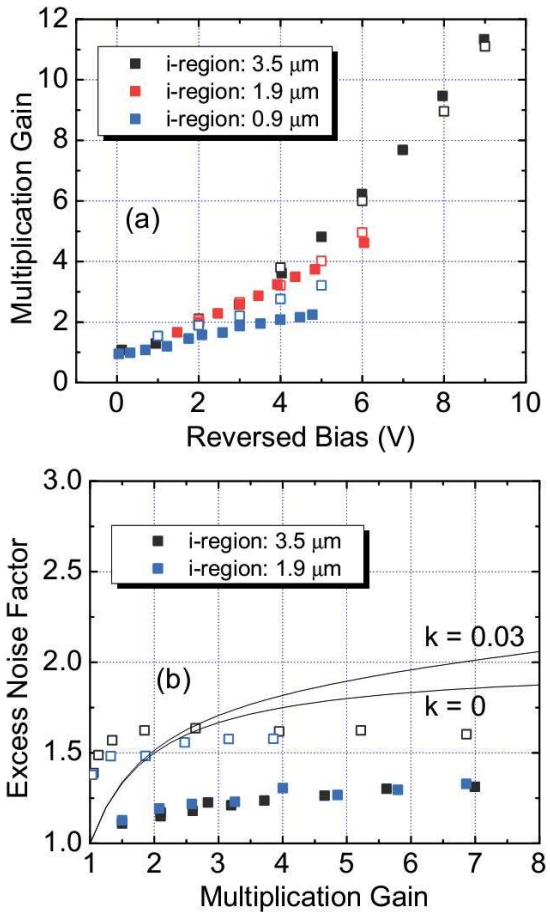

Fig. 2. Simulated (closed symbols) (a) gain and (b) excess noise factor of InAs p-i-n structures with i-region thicknesses of 0.9, 1.9, and 3.5 μm, compared to the measurements in [3] (open symbols).

with the experimental data for all three thicknesses, as shown in Fig. 2(a). The excess noise simulations are consistent with previous measurements on InAs APDs and are in line with pure electron ionization. Figure 3 shows the calculated occupancy percentage of electrons and holes in different valleys of the conduction band. We observe that a significant fraction of electrons populate the satellite valleys (L and X valleys) at low gain, which indicates that electrons in InAs can quickly gain

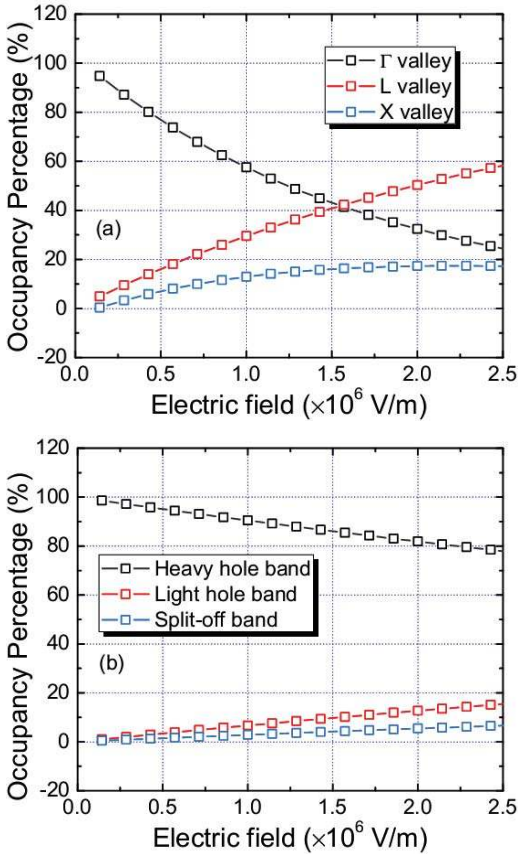

Fig. 3. Simulated occupancy percentage for (a) electrons in Γ, L, and X valleys and (b) holes in heavy-hole, light-hole, and split-off bands at different electric fields.

energy and initiate intervalley scattering or impact ionization. On the other hand, few holes occupy states outside the heavy-hole valance band and their energy increases marginally even at high electric fields. It follows that the ionization coefficient for holes is much lower than that of electrons and therefore k is close to 0, which is consistent with the observation of very low excess noise in InAs APDs. It is also shown by both experiment and simulation in Fig. 2(a) that for a given bias, higher gain is achieved with thicker multiplication region, which suggests that a longer depletion region is preferred for high gain InAs APDs. A thicker depletion region can also effectively suppress the tunneling component of the dark current owing to the thicker effective barrier and lower electric field. Low background doping is crucial to achieve thick depletion regions and gain enhancement. Figure 4 shows the Monte Carlo simulated gain of a p-i-n structure with 6 μm-thick depletion region for different background doping levels. It is clear that lower doping results in significantly higher gain.

III. Growth and Fabrication

Two InAs APD structures with i-region as thick as 6 μm were grown by MBE, as reported in [12]. The schematic cross sections are shown in Fig. 5. Beryllium and silicon were used as acceptors and donors, respectively. Using Hall effect measurement, the extracted n-type background doping concentration in the i-region was below 1×10^{15} cm^{-3}.

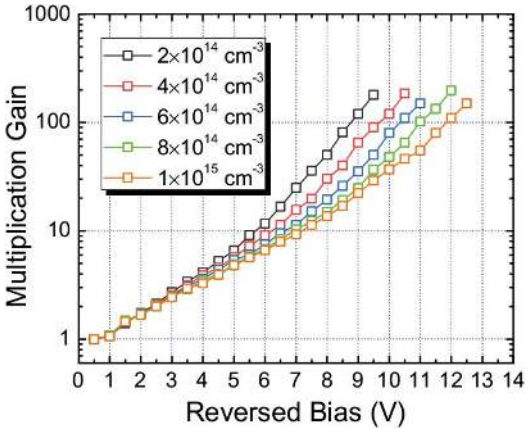

Fig. 4. Simulated gain of a p-i-n structure InAs APD with 6-μm-thick i-region at different background doping levels.

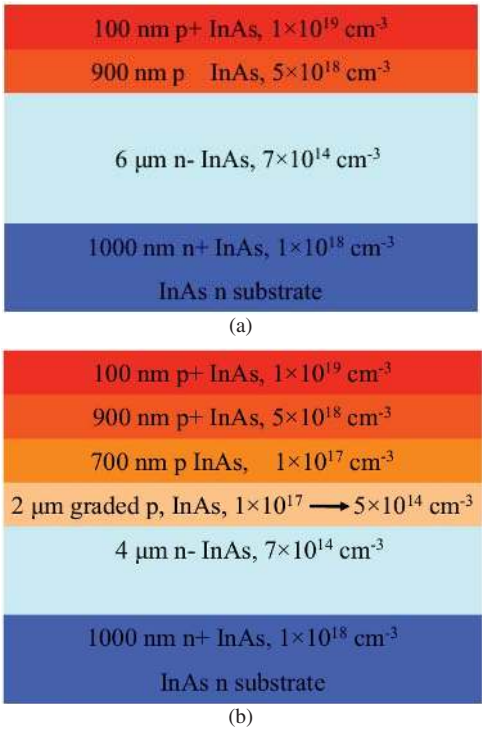

Fig. 5. Layer structure of (a) unintentionally doped (UID) structure and (b) graded p-doped structure (graded).

For the graded p-doped structure, to further reduce the background doping the Be cell temperature was ramped in order to form graded p-type doping in the first 2 μm of the depletion region to compensate the n-type background doping. Mesa structure devices with diameters from 50 μm to 500 μm were defined by wet etching using 1:1:1 (phosphoric acid, hydrogen peroxide, deionised water), followed by 30 seconds etching in 1:8:80 (sulphuric acid, hydrogen peroxide, deionised water). This recipe has been shown to suppress surface leakage current [13]. The etched mesa sidewalls were immediately covered with SU-8 passivation to minimize surface degradation [14]. Due to the small band-gap of InAs, good ohmic contact is easily formed by depositing Ti/Au (20/150 nm) without annealing.

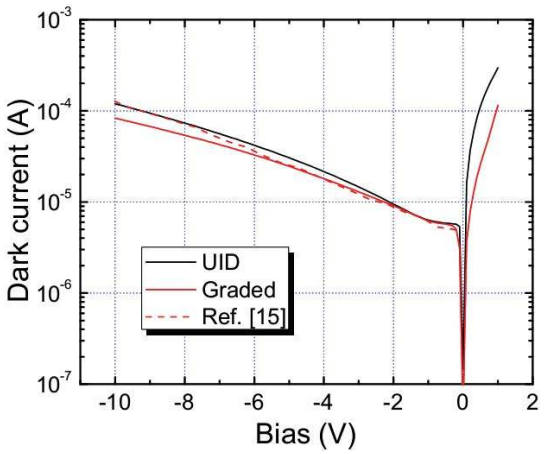

Fig. 6. Measured dark currents of UID and graded structure devices with 100 μm diameter, compared to the data in [16].

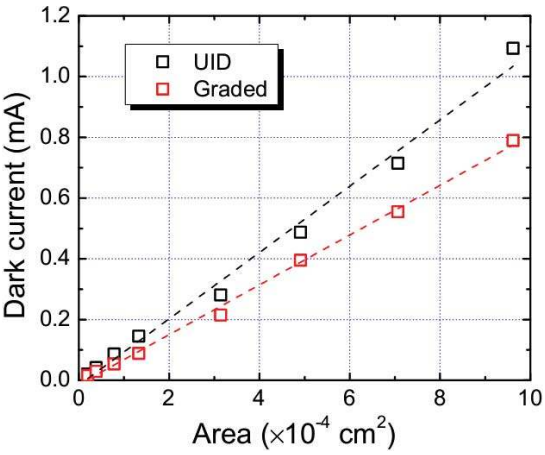

Fig. 7. Dark currents of devices with different areas at bias $= -10$ V for both structures.

IV. Measurement

The dark currents were measured using a HP 4145 B semiconductor parameter analyzer. For gain and excess noise measurement, a phase-sensitive detection method described in [15] was used. The light source was chopped at 200 Hz, then AC photo-current and photo-noise were measured using two lock-in amplifiers. An advantage of this measurement technique is that it enables characterization of photodiodes with high (>1 μA) dark current. Before testing, the sample wafer was cut into very small individual devices to improve heat dissipation. A lensed fiber with light-spot diameter of 20 μm was used to illuminate the device in order to achieve pure-electron injection.

A. Dark Current

Figure 6 shows the measured dark currents of 100 μm-diameter devices for both structures. The dark current of the UID structure is as low as that reported in [16], and even lower dark current is achieved on the graded structure due to reduced diffusion current. The dark currents at -10 V bias of devices with different areas are plotted in Fig. 7. We see that

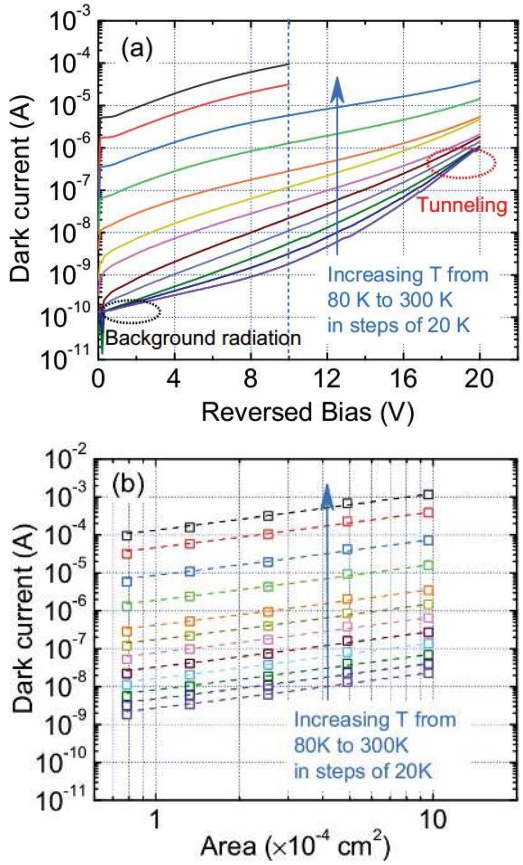

Fig. 8. (a) Dark currents of a 100-μm-diameter graded structure device at different temperatures. (b) Dark currents of devices with different areas at different temperatures, and bias $= -10$ V.

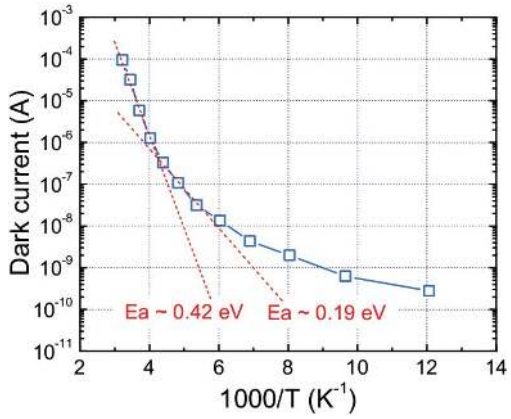

Fig. 9. Dark current at bias $= -10$ V versus $1/kT$ for a 100-μm-diameter graded structure device.

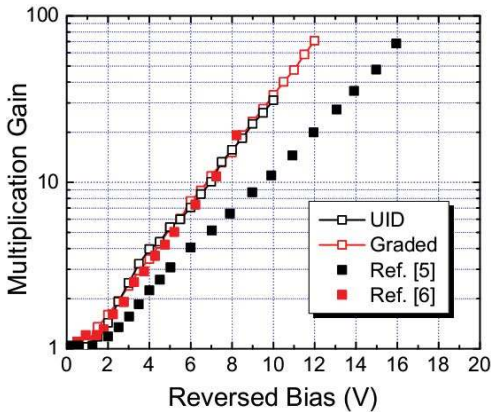

Fig. 10. Measured gain (open symbols) of UID and graded InAs APDs compared to the data in [5] and [6] (closed symbols).

the dark current scales with the active area for both structures, which attests to the efficacy of the SU-8 surface passivation.

Figure 8(a) shows the dark currents of a 100 μm-diameter graded structure APD at different temperatures. The tunneling current does not become significant until the bias exceeds 16 V, which confirms that the 6 μm-thick i-region suppresses the tunneling component of the dark current. The saturation of dark current below 100 K is due to background radiation. Unlike the work in [4], the size-dependent study of dark current in Fig. 8(b) indicates that the dark current of the graded structure InAs APDs is primarily bulk-dominated at all temperatures. Using Eq. 1, an activation energy, E_a, has been extracted from the dark current versus temperature measurement after subtracting the background induced current. In Eq. 1 k is the Boltzmann constant and T is the absolute temperature. As shown in Fig. 9 when T is between 300 K and 220 K, E_a is ~0.42 eV, which is

$$I_d \propto T^2 \exp\left(\frac{-E_a}{kT}\right) \tag{1}$$

close to the band-gap of InAs. In this temperature range the dark current appears to be diffusion current. From 220 K to 140 K, the diffusion current decreases rapidly and can be ignored; the fitted E_a in this temperature range is ~0.19 eV close to mid-gap, an indication that generation-recombination inside the depletion region becomes dominate. The UID structure devices exhibit the same trend except the dark current is slighter higher at all temperatures. Since dark currents for both structures are dominated by diffusion current, one reasonable explanation for the ~20% lower dark current of the graded structure is the slightly thicker p-region due to intentionally graded p-doping. According to the calculation of diffusion current in [6], a thicker p-layer has smaller diffusion current if surface recombination is significant [6], which may be the case since the top surface is not passivated with SU8.

B. Gain and Excess Noise

Figure 10 shows that the measured gain is almost the same for both structures and increases exponentially with bias, showing no sign of breakdown, a signature of k~0. The highest gain that can be measured is limited by the device dark current, which will degrade the measurement accuracy above a certain level (~0.1 mA). For the UID structure the reversed bias was increased up to 10 V before reaching the measurement limit. The highest gain obtained is ~30, while for the graded structure, the slightly lower dark current enables higher bias voltages. The maximum gain, ~70, is achieved at 12 V reversed bias. The InAs APDs in Ref. [6] follow the gain curve of the APDs reported here except the maximum gain is 20. Figure 11 shows that the depletion width for a given

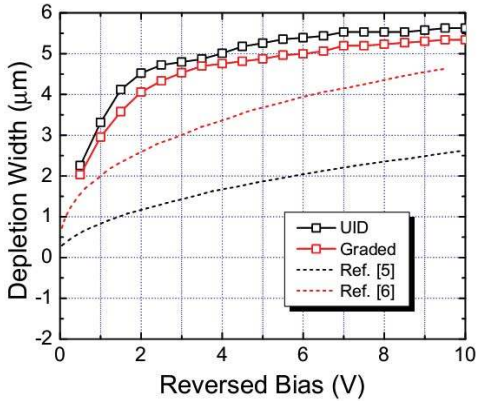

Fig. 11. Depletion region thicknesses of UID and graded InAs APDs compared to the data in [5] and [6] (dash lines).

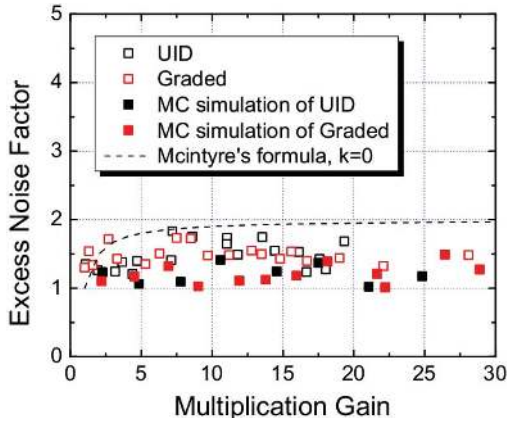

Fig. 12. Measured (open symbols) and simulated (closed symbols) excess noise factor of the UID and graded InAs APDs.

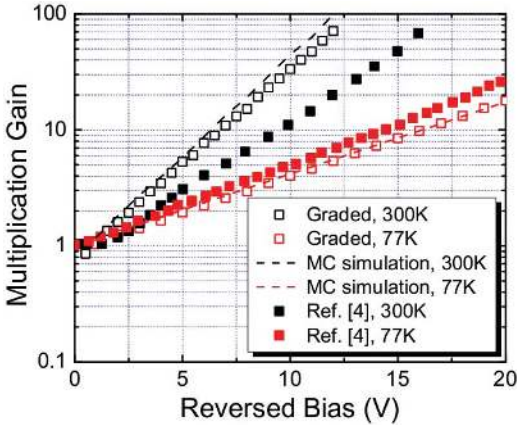

Fig. 13. Measured (open symbols) and simulated (dash lines) gain of the graded structure InAs APD at 77 and 300 K, compared to the data in [4].

bias is almost the same for the UID and graded structures. At high reverse bias, the depletion widths are ~6 μm. We note that comparable depletion width was also reported for the InAs APDs in Ref. [6]. This explains the similarity of the gain curves. On the other hand, the InAs APD in Ref. [5] has a depletion region of approximately 3 μm and the gain increases slowly, i.e., the gain is lower for the same bias, as shown in Fig. 10.

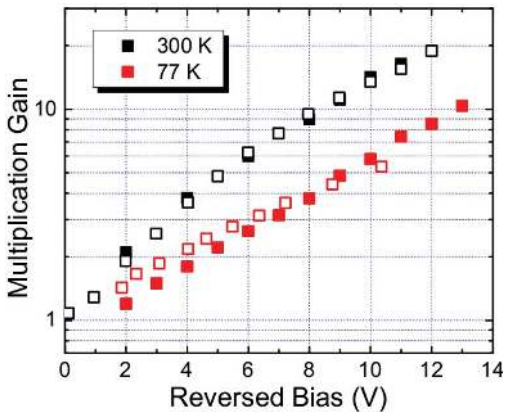

Fig. 14. Measured gain versus bias voltage reported in [7] (open symbols) and simulated (closed symbols) gain of InAs p-i-n structure with 3.5-μm-thick i-region at both 300 and 77 K.

Figure 12 shows the measured and simulated excess noise factor versus gain for the UID and graded structures. These results are also consistent with k~0. The measured gain versus bias voltage of the 6-μm i-region InAs APD in [4] and the graded structure reported here at 77 K are plotted in Fig. 13. Similar to the report in [4], for a given bias voltage the multiplication gain decreases significantly at 77 K, which is opposite to most III-V semiconductors. The gain difference between the structure in [4] and the graded structure here are much smaller at 77 K than at 300 K. This is consistent with the conclusion in Ref. [7], where it was found that unlike at room temperature, at 77 K a thicker depletion region does not result in higher gain because the electron ionization coefficient has stronger dependence on electric field at 77 K. Therefore at 77 K, the gain of the graded structure reported here is only comparable to the gain reported in Ref. [4] even though the graded structure has wider depletion region. To investigate the origin of smaller gain at 77 K, Monte Carlo simulations were performed. Equation 2 [18] was used to model the temperature dependence of the InAs band-gap. The energies of the L and X minima, E_L and E_X, respectively, are assumed to have the same temperature dependence as that of the Γ conduction band minimum, E_Γ [17]. First the model was calibrated by simulation of the InAs p-i-n structure with 3.5 μm thick i-region reported in [7]. As shown in Fig. 14, the simulated gain agrees with the measurement in [7] at 300 K. At 77 K, the increasing rate of gain appears to be slightly different between simulation and measurement; this is probably due to the change of electric

$$E_g = 0.415 - 2.76 \times 10^{-4} \frac{T^2}{T + 83} eV \tag{2}$$

field profile at 77 K since the density of activated dopant varies with temperature, which will result in change of depletion region width, as well as minor change of gain. However, it is difficult to accurately describe this effect in the model. In addition, the increasing rate of gain is only slightly different so this effect should be marginal. With the same set of parameters, simulation was then performed on the graded APD structure and, again, there is good agreement between experiment and simulation, see Fig. 13.

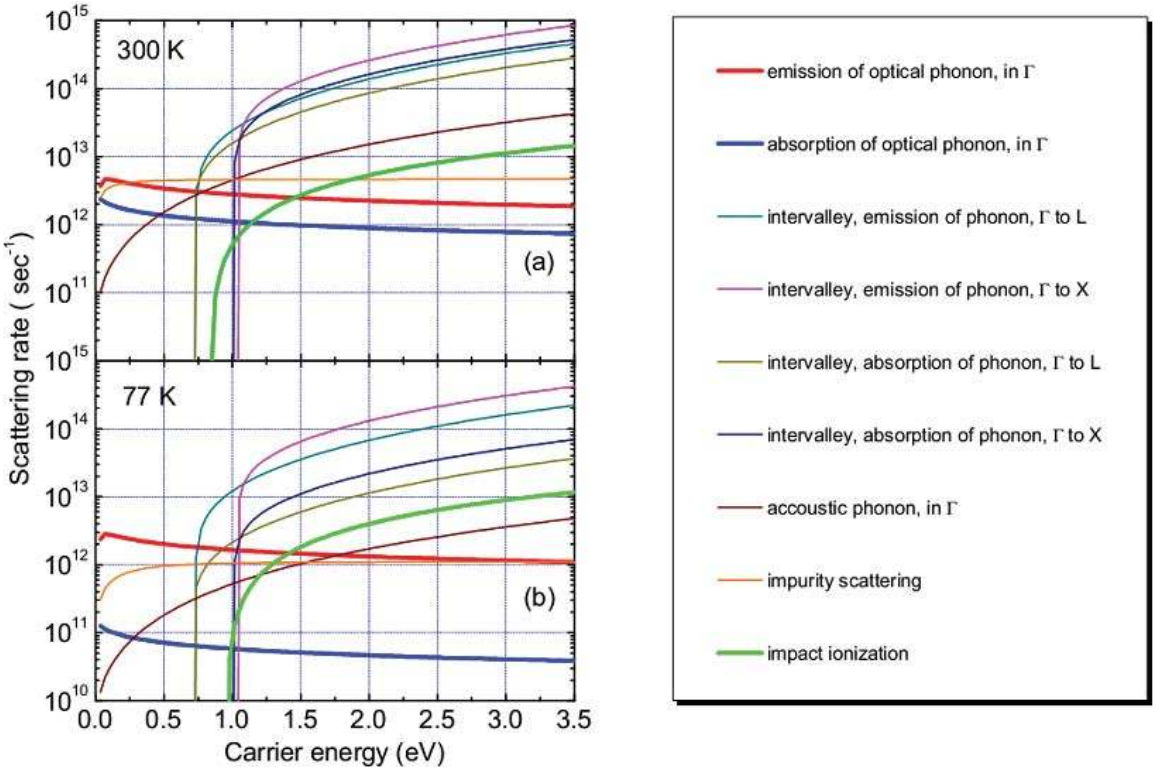

Fig. 15. Calculated electron scattering rates in an InAs APD at (a) 300 and (b) 77 K.

As the temperature decreases, the total carrier scattering rates decrease significantly. Consequently, the carriers will experience less phonon scattering and gain energy faster, however, the bangap, and thus, the threshold energy for impact ionization increase at lower temperature, making it harder for carriers to initiate impact ionization events. For typical III-V materials, such as InP, InAlAs, and GaAs the first mechanism is more pronounced and higher gain is expected with decreasing temperature. On the other hand, InAs exhibits the opposite. If we look at the simulated electron scattering rates (Fig. 15) for different scattering mechanisms, there are basically two regions: 1) when the electron energy is <1 eV, intervalley scattering due to non-polar optical phonons is marginal and electrons will primarily stay in the Γ valley. In this energy regime, impurity and polar optical phonon scattering dominate. Since polar optical phonon scattering involves emission or absorption of optical phonons, we focus on phonon scattering for this case. 2) On the other hand, when the electron energy is >1 eV, intervalley scattering and impact ionization rates increase rapidly. For an APD, the impact ionization coefficients depend on how fast a carrier can attain threshold energy, and, for electrons, the two most important processes are 1) phonon-scattering at energy <1eV, which determines the rate of increase of energy and 2) the impact ionization scattering rate, which determines the threshold energy and the electron ionization rate, or simply the "destination" of electron energy. In Fig. 15, when the electron energy is <1 eV, although impurity scattering is smaller at 77 K than at 300 K, we note that the optical phonon emission rate remains almost unchanged. Thus, in InAs the electrons still experience numerous phonon scattering events at 77 K. In addition, the absorption of optical phonons decreases dramatically due to the significantly decreased number of phonons according to the Bose-Einstein distribution (see Eq. 3). Hence it becomes harder for electrons to gain energy

$$\langle n \rangle = \frac{1}{\exp(\frac{\hbar\omega}{kT}) - 1}. \tag{3}$$

The influence of higher threshold energy that results from the larger band-gap at 77 K causes the ionization coefficient of the electron to decrease, resulting in the smaller gain observed in Fig. 14 at 77 K. The low gain at 77 K appears to restrict the operation of these APDs to the temperature range of 200 K to 300 K, which can be achieved with two- or three-stage thermoelectric coolers.

C. Gain-Bandwidth Product

The bandwidth was measured with a HP 20 GHz lightwave component analyzer. Figure 16 shows the measured frequency response for various bias voltages (open symbols) of a 70 μm-diameter graded structure device that was bonded to a 50 Ω G-S-G contact pad. The measured bandwidth is in the range 2 GHz to 3 GHz independent of bias voltage. By measuring the S-parameters, the total resistance and capacitance of the device under test were determined to be around 58 Ω and 0.18 pF, respectively, which yields a RC-limited bandwidth ~15 GHz. Therefore, the measured 3 dB bandwidth of device is actually limited by carrier transit-time. Monte Carlo simulation using the method described in [8] was employed to verify the transit-time response. Impulse responses are plotted in Fig. 17. The pulse widths at different bias are nearly the same.

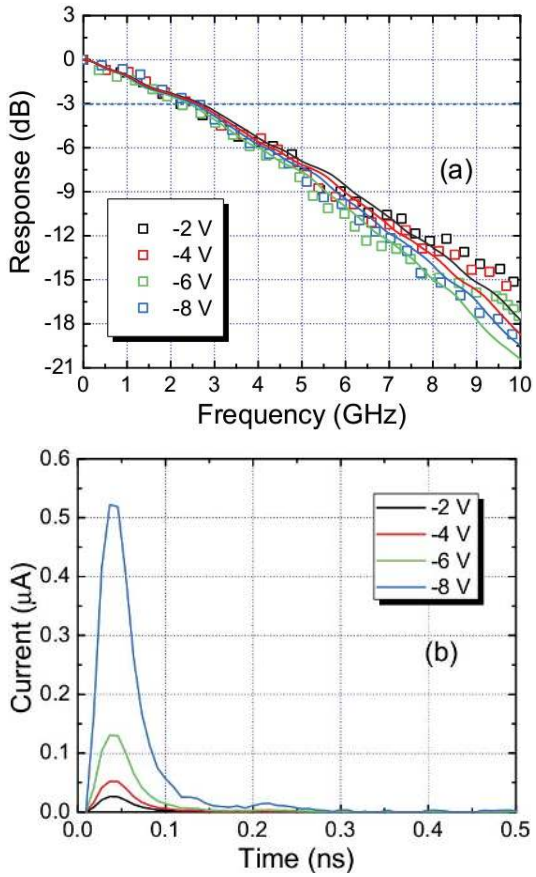

Fig. 16. (a) Measured (dots) and simulated (lines) frequency responses of the graded structure InAs APD at bias $= -2, -4, -6$, and -8 V. (b) Simulated impulse responses of the graded structure InAs APD.

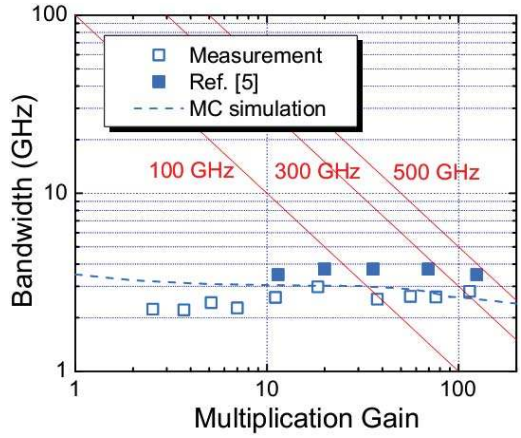

Fig. 17. Measured (open symbol) and simulated (dashed line) bandwidths of the graded structure InAs APD, compared to the data in [5].

The frequency responses, shown as solid lines in Fig. 16, are the Fourier transform of the impulse responses. Since the speed is limited by the transit time, a shorter depletion region is required to speed up carrier transport, however, as indicated by the simulated gain curves in Fig. 2(a) a shorter depletion region has lower gain for a given voltage. Increasing the voltage to recover the gain will result in higher dark current, particularly if tunneling becomes significant. Although the bandwidths of the thick depletion layer APDs may be too restrictive for telecommunication applications, they may be sufficient for some imaging systems, where bandwidths of several GHz are widely used. The measured and simulated bandwidths versus gain are plotted in Fig. 17. Consistent with the measurements reported in [5] there is no evidence of a finite gain-bandwidth product, as would be expected for k~0.

V. Conclusion

In this paper, we report two InAs APDs with ~6 μm-thick multiplication region and a Monte Carlo simulation tool for InAs APDs. These APDs exhibit low dark current and gain as high as 70 at room temperature and 12 V bias. The bandwidth is transit-time limited in the range 2 to 3 GHz independent of gain. The performance has also been simulated with a Monte Carlo model. Good agreement between measurements and simulations has been achieved. Low temperature measurements indicate the gain of InAs APDs decreases significantly with temperature, using Monte Carlo simulation, we concluded that this is caused by high emission of optical phonons and higher threshold energy for impact ionization at low temperature.

Acknowledgment

The authors would like to thank Prof. J. P. R. David, Dr. C. H. Tan, and J. Green, University of Sheffield, Sheffield, U.K., for their assistance with equipment set-up and helpful discussions.

References

[1] R. C. J. McIntyre, "Multiplication noise in uniform avalanche photodiodes," *IEEE Trans. Electron. Devices*, vol. 13, no. 1, pp. 164–168, Jan. 1966.

[2] A. R. J. Marshall, C. H. Tan, M. J. Steer, and J. P. R. David, "Extremely low excess noise in InAs electron avalanche photodiodes," *IEEE Phton. Tech. Lett.*, vol. 21, no. 13, pp. 866–868, Jul. 2009.

[3] A. R. J. Marshall, J. P. R. David, and C. H. Tan, "Impact ionization in InAs electron avalanche photodiodes," *IEEE Trans. Electron. Devices*, vol. 57, no. 10, pp. 2631–2638, Oct. 2010.

[4] P. J. Ker, A. R. J. Marshall, J. P. R. David, and C. H. Tan, "Low noise high responsivity InAs electron avalanche photodidoes for infrared sensing," *Phys. Status. Solidi C*, vol. 9, no. 2, pp. 310–313, 2011.

[5] A. R. J. Marshall, P. J. Ker, A. Krysa, J. P. R. David, and C. H. Tan, "High speed InAs electron avalanche photodiodes overcome the conventional gain-bandwidth product limit," *Opt. Exp.*, vol. 19, no. 23, pp. 23341–23349, Nov. 2011.

[6] A. R. J. Marshall, A. Krysa, S. Zhang, A. S. Idris, S. Xie, J. P. R. David, and C. H. Tan, "High gain InAs avalanche photodiodes," in *Proc. 6th Int. EMRS DTC Tech. Conf.*, 2009, pp. 1–4.

[7] A. R. J. Marshall, P. Vines, P. J. Ker, J. P. R. David, and C. H. Tan, "Avalanche multiplication and excess noise in InAs electron avalanche photodiodes at 77K," *IEEE J. Quantum Electron.*, vol. 47, no. 6, pp. 858–864, Jun. 2011.

[8] W. Sun, X. Zheng, Z. Lu, and J. C. Campbell, "Monte carlo simulation of InAlAs/InAlGaAs tandem avalanche photodiodes," *IEEE J. Quantum Electron.*, vol. 48, no. 4, pp. 528–532, Apr. 2012.

[9] W. Sun, X. Zheng, Z. Lu, and J. C. Campbell, "Monte carlo simulation of $Al_xGa_{1-x}As (x > 0.6)$ avalanche photodiodes," *IEEE J. Quantum Electron.*, vol. 47, no. 12, pp. 1531–1536, Dec. 2011.

[10] L. V. Keldysh, "Kinetic theory of impact ionization in semiconductors," *Soviet Phys. JETP*, vol. 37, no. 10, pp. 509–518, 1960.

[11] H. Arabshahi and S. Golafrooz, "Monte carlo based calculation of electron transport properties in bulk InAs, AlAs and InAlAs," *Bulg. J. Phys.*, vol. 37, no. 4, pp. 215–222, 2010.

[12] S. J. Maddox, W. Sun, Z. Lu, H. P. Nair, J. C. Campbell, and S. R. Bank, "Enhanced low-noise gain from InAs avalanche photodiodes with reduced dark current and background doping," *Appl. Phys. Lett.*, vol. 101, no. 15, pp. 151124–151127, 2012.

[13] A. R. J. Marshall, C. H. Tan, J. P. R. David, M. J. Steer, and M. Hopkinson, "Growth and fabrication of InAs APDs," in *Proc. 4th EMRS DRC Tech. Conf.*, 2007, pp. 1–5.
[14] H. S. Kim, E. Plis, A. Khoshakhlagh, S. Myers, N. Gautam, Y. D. Sharma, L. R. Dawson, S. Krishna, S. J. Lee, and S. K. Noh, "Performance improvement of InAs/GaSb strained layer super-lattice detectors by reducing surface leakage current with SU-8 passivation," *Appl. Phys. Lett.*, vol. 96, no. 3, pp. 033502-1–033502-3, 2010.
[15] K. S. Lau, C. H. Tan, B. K. Ng, K. F. Li, R. C. Tozer, J. P. R. David, and G. J. Rees, "Excess noise measurement in avalanche photodiodes using a transimpedance amplifier front-end," *Meas. Sci. Technol.*, vol. 17, no. 7, p. 1941, Jul. 2006.
[16] P. J. Ker, A. R. J. Marshall, A. B. Krysa, J. P. R. David, and H. T. Chee, "Temperature dependence of leakage current in InAs avalanche photodiodes," *IEEE J. Quantum Electron.*, vol. 47, no. 8, pp. 1123–1128, Aug. 2011.
[17] C. H. Tan, G. J. Rees, P. A. Houston, J. S. Ng, W. K. Ng, and J. P. R. David, "Temperature dependence of electron impact ionization in In0.53Ga0.47As," *Appl. Phys. Lett.*, vol. 84, no. 13, pp. 2322–2325, 2004.
[18] Z. M. Fang, K. Y. Ma, D. H. Jaw, R. M. Cohen, and G. B. Stringfellow, "Photoluminescence of InSb, InAs, and InAsSb grown by organometallic vapor phase epitaxy," *J. Appl. Phys.*, vol. 67, no. 11, pp. 7034–7039, 1990.

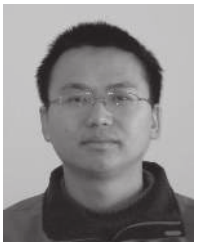

Wenlu Sun was born in Puyang, China, in 1989. He received the B.S. degree in physics from the University of Science and Technology of China, Hefei, China, in 2009. He is currently pursuing the Ph.D. degree with the Department of Electrical Engineering, University of Virginia, Charlottesville.

His current research interests include low-noise avalanche photodiodes and single-photon counting.

Zhiwen Lu received the B.S. degree in physics from the University of Science and Technology of China, Anhui, China, in 2007, and the M.E. degree in electrical engineering from the University of Virginia, Charlottesville, in 2009. She is currently pursuing the Ph.D. degree in electrical engineering with the University of Virginia.

Her current research interests include infrared single photon avalanche diodes, low noise avalanche photodiodes, and quantum dots infrared photodiodes.

Xiaoguang Zheng received the B.S.E.E. degree from the Beijing Institute of Technology, Beijing, China, in 1985, the M.S. degree in electrical engineering from the Hebei Semiconductor Research Institute, Anhui, China, in 1991, and the Ph.D. degree in electrical engineering from the University of Texas at Austin, Austin, in 2003.

His current research interests include optoelectronic devices: impact ionization properties of III-V compound materials, high-speed long-wavelength avalanche photodiodes and arrays, and heterogeneous material integration via direct wafer bonding.

Joe C. Campbell (S'73–M'74–SM'88–F'90) received the B.S. degree from the University of Texas at Austin, Austin, in 1969, and the M.S. and Ph.D. degrees from the University of Illinois at Urbana-Champaign, Champaign, in 1971 and 1973, respectively, all in physics.

He was with Texas Instruments, Dallas, where he was engaged in research on integrated optics, from 1974 to 1976. In 1976, he joined the AT&T Bell Laboratories, Holmdel, NJ, as a Staff Member, where he was involved in research on a variety of optoelectronic devices, including semiconductor lasers, optical modulators, waveguide switches, photonic integrated circuits, and photodetectors, with emphasis on high-speed avalanche photodiodes for high-bit-rate lightwave systems. In 1989, he joined the University of Texas at Austin as a Professor of electrical and computer engineering and as the Cockrell Family Regents Chair in Engineering. In 2006, he became a Faculty Member with the University of Virginia, Charlottesville, and then the Lucian Carr and the III Chair of Electrical Engineering and Applied Science. He has co-authored 320 papers for refereed technical journals, more than 200 conference presentations, and 6 book chapters. His research focused on the optoelectronic components that are used to generate, modulate, and detect the optical signals. His current research interests include single-photon-counting avalanche photodiodes, Si-based optoelectronics, high-speed low-noise avalanche photodiodes, ultraviolet photodetectors, and quantum-dot IR imaging.

Scott. J. Maddox received the B.S. and M.S. degrees from The University of Texas at Austin, Austin, in 2009 and 2011, respectively, where he is currently pursuing the Ph.D. degree, all in electrical engineering.

His current research interests include MBE growth and characterization of dilute-bismuthide alloys for photodetector applications, InAs APDs, and epitaxial plasmonic materials.

Hari P. Nair received the B.Tech. degree from the Indian Institute of Technology, Chennai, India, in 2006, the M.S. degree from The University of Texas at Austin, Austin, in 2008. He is currently pursuing the Ph.D. degree.

His current research interests include developing molecular beam epitaxy (MBE) grown GaSb-based dilute-nitride alloys for type-I diode lasers operating in the 3–5 μm wavelength range, their thermal annealing characteristics and MBE growth of rare earth monopinictide nanoparticle enhanced tunnel junctions.

Mr. Nair received a Student Paper Award at Electronics Materials Conference.

Seth R. Bank (S'95–M'06–SM'11) received the B.S. degree from the University of Illinois at Urbana-Champaign (UIUC), Urbana, in 1999, and the M.S. and Ph.D. degrees from Stanford University, Stanford, CA, in 2003 and 2006, all in electrical engineering. While at UIUC, he studied the fabrication of InGaP–GaAs and InGaAs–InP HBTs. His Ph.D. research focused upon the MBE growth, fabrication, and device physics of long-wavelength VCSELs and low-threshold edge-emitting lasers in the GaInNAs(Sb)–GaAs material system.

He was a Post-Doctoral Scholar with the University of California, Santa Barbara, in 2006, where his research centered on the growth of metal-semiconductor hetero- and nano-structures (ErAs nanoparticles in GaAs). In 2007, he joined the University of Texas at Austin, Austin, where he is currently an Associate Professor of electrical and computer engineering and holder of the fifth Temple Foundation Endowed Faculty Fellowship. His current research interests include the MBE growth of novel heterostructures and nanocomposites and their device applications. He has co-authored over 175 papers and presentations.

Dr. Bank was the recipient of the 2010 Young Investigator Program Award from ONR, the 2010 NSF CAREER Award, the 2009 Presidential Early Career Award for Scientists and Engineers nominated by ARO, the 2009 Young Investigator Program Award from AFOSR, the 2009 Young Scientist Award from the International Symposium on Compound Semiconductors, the 2008 DARPA Young Faculty Award, the 2008 Young Investigator Award from the North American MBE Meeting, and several best paper awards.